Accelerated Publications

Structure of Influenza Virus Neuraminidase B/Lee/40 Complexed with Sialic Acid and a Dehydro Analog at 1.8-Å Resolution: Implications for the Catalytic Mechanism†

Musiri N. Janakiraman,‡,§,‖ Clinton L. White,‡,⊥ W. Graeme Laver,# Gillian M. Air,§ and Ming Luo*,‡,§,⊥

Center for Macromolecular Crystallography, Department of Microbiology, and Department of Biochemistry and Molecular Genetics, University of Alabama at Birmingham, Birmingham, Alabama 35294, and John Curtin School of Medical Research, Australian National University, Canberra 260, Australia

Received March 29, 1994; Revised Manuscript Received May 16, 1994•

ABSTRACT: Neuraminidase is one of the two glycoprotein spikes protruding from the influenza virus membrane. We have determined by X-ray crystallography the native structure of B/Lee/40 neuraminidase (NA) and the structures of its crystals soaked with a substrate, *N*-acetylneuraminyllactose (NANL), and an inhibitor, 2-deoxy-2,3-didehydro-*N*-acetylneuraminic acid (DANA) at 1.8-Å resolution. NANL was hydrolyzed by the crystalline NA to generate the product *N*-acetylneuraminic acid (NANA, also known as sialic acid), which is still able to bind to NA. In the difference Fourier map of the presumed NA–NANA complex, the moiety bound in the active site had a distorted boat conformation of NANA, but there is no significant electron density for O2. The structure of the bound moiety is not identical to that of chemically synthesized DANA soaked into NA crystals. Prolonged incubation of NANA with NA in solution at room temperature produced only a trace amount of DANA as detected by NMR. On the basis of our studies, a mechanism is proposed for the enzymatic hydrolysis by influenza virus neuraminidase.

The surface antigens found on the membrane envelope of influenza virus are two glycoproteins, hemagglutinin and neuraminidase (EC 3.2.1.18, acylneuraminyl hydrolase). The tetrameric neuraminidase catalyzes the hydrolysis of the α-(2,3) or α-(2,6) glycosidic linkage between a terminal sialic acid and its adjacent carbohydrate moiety on a variety of glycoconjugates. In general, enzyme-catalyzed hydrolysis of biopolymers requires (i) a nucleophile (which may be an "activated water" molecule) or a proton donor from the enzyme to induce the formation of a transition-state intermediate, (ii) a pocket to bind the specific substrate, and (iii) one or more residues to stabilize the transition-state intermediate. On the basis of the structural analysis of the A/Tokyo/3/67 NA–NANA[1] complex, Varghese et al. (1992) implicated an aspartic acid at position 152 in the catalysis. However, this aspartic side chain is solvent exposed and, therefore, has a pK_a of 3.9, which is inconsistent with the pH range (4.5–9.0) of NA activity.

In this paper, we present the crystal structure of B/Lee/40 influenza virus neuraminidase and its complexes with presumed NANA and DANA at 1.8-Å resolution. The binding of DANA to NA ($K_i \approx 5\times 10^{-6}$ M) is about 1000-fold higher than that of NANA, and DANA has been considered as a transition-state analogue for sialic acid cleavage (Meindl et al., 1971). Burmeister et al. (1993) described the crystal

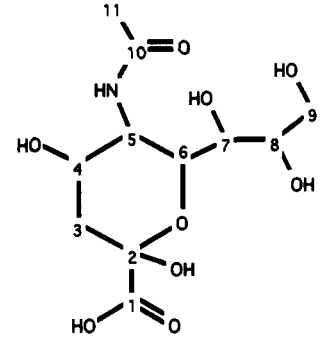

NANA
N-acetyl neuraminic acid
(*α-sialic acid*)

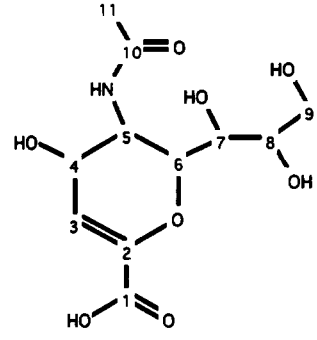

DANA
2-deoxy-2,3-didehydro-N-acetyl neuraminic acid

† This project was supported by NIH Grants AI-31888 to M.L. and AI-26718 to G.M.A.

* Author to whom correspondence should be addressed.
‡ Center for Macromolecular Crystallography, University of Alabama at Birmingham.
§ Department of Microbiology, University of Alabama at Birmingham.
‖ Current address: The Upjohn Co., Kalamazoo, MI 49001.
⊥ Department of Biochemistry and Molecular Genetics, University of Alabama at Birmingham.
Australian National University.

• Abstract published in *Advance ACS Abstracts,* June 15, 1994.

[1] Abbreviations: NA, neuraminidase; NANA, *N*-acetylneuraminic acid; DANA, 2-deoxy-2,3-didehydro-*N*-acetylneuraminic acid; NANL, *N*-acetylneuraminyllactose; K_i, inhibition constant; F_o, observed structure factor; F_c, calculated structure factor; SA, simulated annealing; NAG, *N*-acetylglucosamine.

0006-2960/94/0433-8172$04.50/0

Table 1: Crystallographic Data for Native B/Lee/40 NA and Complex I and Complex II

							overall
NA (Native): $a = b = 124.56$ Å, $c = 71.66$ Å; Tetragonal Space Group $P42_12$							
resolution shell, Å	4.16	2.94	2.40	2.08	1.86	1.76	1.76
no. of reflections	3846	7035	6729	5564	3746	1132	28052
completeness, %	95.6	95.4	70.4	49.5	29.2	13.9	52.4
R_{sym}, %[a]	8.3	12.7	20.4	27.5	36.5	40.1	12.2
Complex I (NA–NANA): $a = b = 125.29$ Å, $c = 72.04$ Å; Tetragonal Space Group $P42_12$							
resolution shell, Å	4.23	3.00	2.45	2.12	1.90	1.78	1.78
no. of reflections	3757	6879	7540	7157	5486	1511	32330
completeness, %	95.8	97.3	82.0	65.2	45.2	16.1	61.4
R_{sym}, %	7.0	11.1	19.0	20.7	22.0	21.2	12.6
Complex II (NA–DANA): $a = b = 124.45$ Å, $c = 71.61$ Å; Tetragonal Space Group $P42_12$							
resolution shell, Å	3.18	2.52	2.21	2.00	1.86	1.77	1.77
no. of reflections	3829	7014	6432	3999	2691	755	24720
completeness, %	94.7	94.7	67.0	35.4	20.9	5.4	47.1
R_{sym}, %	9.0	14.2	22.1	41.5	36.9	36.4	13.5

[a] $R_{sym} = 100(\Sigma|I_i - \langle I\rangle|/\Sigma I_i)$, where ΣI_i is the sum of all observations of all reflections within the resolution shell.

Table 2: Refinement Statistics for Native NA and Complex I and Complex II

		NA–NANA			
	native NA	model 1	model 2	model 3	NA–DANA
no. of non-hydrogen atoms	3181	3202	3201	3201	3201
no. of reflections	27321	31545	31545	31545	23998
R-factor, %[a]	20.1	20.4	19.9	19.9	21.1
$\langle B\rangle$, Å^2	21.0	10.6	10.7	10.6	19.3
rms deviation from ideality					
bond distance, Å	0.012	0.013	0.014	0.014	0.012
bond angle, deg	1.356	1.315	1.359	1.348	1.433
dihedral angle, deg	28.045	28.052	27.863	27.908	28.957
improper angle, deg	2.254	2.174	2.073	2.169	2.491

[a] R-factor $= 100(\Sigma\|\|F_o| - |F_c\|\|/\Sigma|F_o|)$.

structure of influenza virus neuraminidase B/Beijing/1/87 soaked in NANL. The authors concluded that the moiety bound in the active site was not NANA, but DANA. They suggested that DANA was a side product produced at a low rate during the neuraminidase hydrolytic reaction. Our experimental data have shown some different results which will be discussed in detail in this paper.

MATERIALS AND METHODS

Structure Determination. Crystals of B/Lee/40 influenza virus neuraminidase were prepared following Lin et al. (1990). Complex I was obtained by soaking a crystal of NA overnight at room temperature in 5.0 mM NANL (Sigma Chemical Co.) in mounting solution [20% (w/v) PEG 3350, 0.16 M NaCl, pH 6.6]. Complex II was prepared by soaking a crystal of NA overnight in 5.0 mM DANA (Boehringer Mannheim) in the same mounting solution. X-ray diffraction data of the native and complex crystals were recorded on a Siemens area detector at room temperature using Cu Kα radiation from a Rigaku RU-200 rotating anode generator operating at 40 kV and 100 mA. The data collection parameters were crystal to detector distance 12.5 cm, swing angle 30°, exposure time 10 min per frame, and a frame width of 0.25°. The data thus collected (400 frames) were processed by the XENGEN (Howard et al., 1985) and CCP4 (CCP4, 1979) packages. Only reflections for which $I/\sigma_I \geq 1$ were included (Table 1). For the structure determination of the native B/Lee/40 NA, we used the atomic coordinates of B/Beijing/1/87 NA (Burmeister et al., 1992) (94% amino acid identity to B/Lee/40 NA) and our earlier F_o data set at 2.4-Å resolution (statistics not shown) to obtain the initial atomic model by the molecular replacement method (Rossmann & Blow, 1962). An $\|F_o| - |F_c\|$ difference map was calculated after all atoms of the 21 different side chains were removed. The differing side chains and altered main-chain atoms were modeled into the difference density using FRODO (Jones, 1985). Three rounds of PROSLQ (Hendrickson & Connert, 1981) refinement at 3.0-Å resolution and model building led to a structure with an R-factor of 22%. One more round of PROLSQ using all data to 2.4-Å resolution resulted in a structure with an R-factor of 24%. Subsequently, after ten cycles of rigid body refinement, a full cycle of simulated annealing (SA) refinement at 1.8-Å resolution was carried out using X-PLOR (Brunger, 1992). An $\|F_o| - |F_c\|$ map was then calculated to locate one *N*-acetylglucosamine (NAG) residue (attached to Asn 284) and 125 well-defined water molecules. This resulting structure (390 amino acid residues, 1 NAG residue, 2 Ca^{2+} ions, and 125 water molecules per monomer) served as the native model for the refinement of the two complexes to 1.8-Å resolution. $\|F_o| - |F_c\|$ maps were used to place the inhibitor molecule in the enzyme active site prior to the SA refinements using X-PLOR. During such refinement runs of complex I, three different starting models were used for the molecule in the active site: model 1, NANA in its α-boat conformation; model 2, NANA in its α-boat conformation but without O2; and model 3, DANA. Restraints on the dihedral angles C2–C3–C4–C5 and C5–C6–O6–C2 and the improper angles C2–O6–O2–C3 (model 1 only), C2–C1–O6–C3, and C3–H31 (H3 in the case of model 3)–C2–C4 were removed to allow for any change of geometry about C2. The crystallographic R-factors are those obtained after individual temperature factor refinement using X-PLOR. Complex II was refined using exactly the same conditions as complex I, model 3. The final analysis of the structure refinement is presented in Table 2.

NMR Analysis of NA Products. Experiments were designed to detect if DANA is one of the products in hydrolysis

FIGURE 1: Ribbon drawing of a monomer of B/Lee/40 influenza virus neuraminidase using RIBBONS (Carson, 1987). The yellow spheres represent amino acid residues which differ from all other type B neuraminidases sequenced. The view is down the tetramer 4-fold axis which is passing through Ca^{2+} 501. The disulfide bridges, structural Ca^{2+} ion binding site (Ca^{2+} 500), NAG binding site (N284), and sialic acid binding site are all highlighted.

by influenza virus neuraminidase. Since sialic acid is a substrate of viral neuraminidase (Burmeister et al., 1993) in the sense that the hydroxyl group at the C2 position is released during the formation of the oxocarbonium intermediate, it was used as the substrate in our studies. NANA (10 mM) was incubated with NA in solution (40 nM or 10 μM) at 22 °C for 48 h. The solution was then filtered through a Centricon (Amicon) apparatus to remove NA, and water was replaced by D_2O through repetitive lyophilization. The sample was then analyzed by NMR spectroscopy on a 600-MHz machine (Bruker). Controls of pure NANA, DANA, and a mixture of 1:1000 DANA/NANA were also scanned.

Hydration of DANA by NA. A 1-mL volume of the DANA solution (10 mM DANA, 0.5 M phosphate buffer, pH 6.0) was incubated with either B/Lee/40 NA (0.5, 1, or 2 mg) or A/tern/Australia/G70c/75 NA (2 mg). Aliquots were taken out at given times, and the production of NANA was measured by the method of Aymard-Henry et al. (1973).

RESULTS

What Binds in the Active Site? Influenza virus neuraminidase is a tetramer made up of identical subunits, and each monomer has six twisted β-sheets of four antiparallel strands arranged as a propeller. The active site is a crater located near the center of the monomer (Figure 1). The difference Fourier maps for complex I and complex II showed clear electron densities occupying the active site. With the exception of O2, all the non-hydrogen atoms of NANA could be fitted into the difference electron density in complex I. There is no density for O2 at a contour level of 1.0σ. The lack of O2 density cannot be an artifact because the densities corresponding to O4, O7, O8, and O9 are clearly present. A separate difference Fourier map (not shown) between F_o's of complex I and F_c's calculated using the refined coordinates of complex I, model 2, did not show any significant electron density corresponding to O2. Thus the moiety bound in complex I seems to be a distorted form of α-sialic acid without the OH2 hydroxyl group (Figure 2), as was observed by Burmeister et al. (1993). In complex II, all the non-hydrogen atoms of DANA could be fitted into the difference electron density.

There is a possibility that the moiety bound in complex I is DANA, which could be produced by the loss of a proton at the C3 position of NANA during the glycosidic cleavage reaction. DANA could also be formed by a nonspecific β-elimination with the participation of acidic and basic residues on the surface of the enzyme. In fact, a trace amount (<0.1%) of DANA was detected by NMR analyses when NANA was incubated with NA in solution over 48 h at room temperature (Figure 3).

The conversion of NANA to DANA by neuraminidase was also reported by Burmeister et al. (1993), but the experimental conditions and results were somewhat different. In contrast to their crystallographic studies which were done at room temperature or 4 °C, Burmeister et al. (1993) incubated NANL with NA in solution for 36 h at 37 °C. Samples were then derivatized by bis(trimethylsilyl)trifluoroacetamide for 3 h, and DANA production was measured by coupled gas chromatography/mass spectrometry. No DANA was detected when the NA:NANL ratio was 1:12 500. When the enzyme:substrate ratio was raised to 1:25 (500-fold increase of NA), a significant amount of DANA was detected.

The solution incubation experiments, as well as the crystallographic experiments, presented here were done at room temperature (≈22 °C). Only a trace amount of DANA was produced (<1:1000 DANA:NANA ratio) at an enzyme:

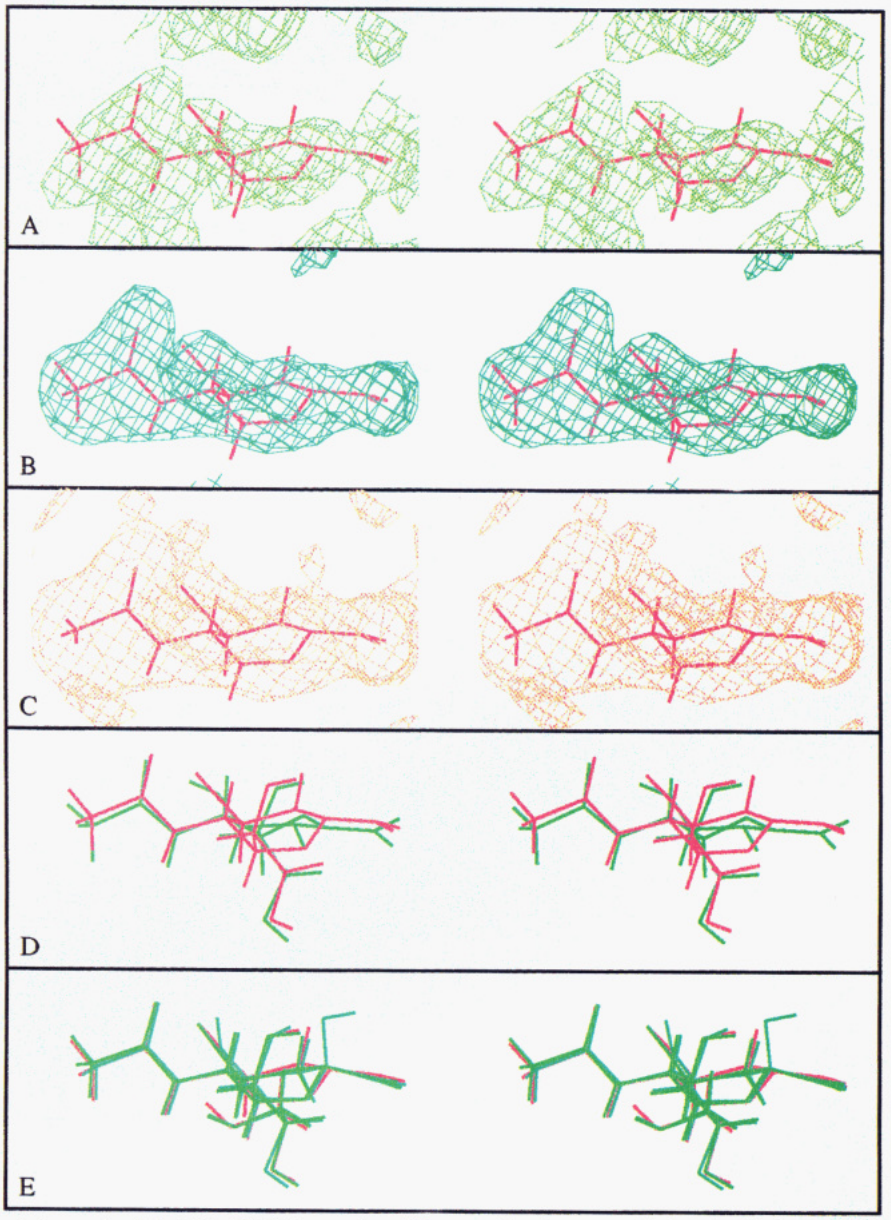

FIGURE 2: (A) Stereo photograph of the NA–NANA complex difference Fourier map calculated with the coefficients $|2|F_o| - |F_c||$ using the refined native coordinates only. A total of 31 545 unique reflections up to 1.8-Å resolution were used for this calculation, and the electron density map is contoured at the 1.0σ level. The density corresponding to the glycerol group was left out for clarity. (B) $\|F_o| - |F_c\|$ map contoured at the 1.0σ level calculated by the same routine as in (A) but using the refined model 3 complex coordinates. (C) Same map as in (B) contoured at the 0.5σ level. (D) Superposition of the refined model 3 (red) and DANA (green) as bound in the active site of NA to compare the geometry of C2 in the two complexes. (E) Superposition of the three refined NANA models: model I (blue), model II (green), and model III (red).

substrate ratio of either 1:250 000 or 1:1000 (Figure 3). An increase of the enzyme:substrate ratio by 250-fold did not change the yield of DANA under these conditions. Since the ratio of DANA:NANA in solution should be equal to the ratio of DANA:NANA in the solvent volume of crystalline NA, NANA should compete equally for the NA active site in the crystal even though the affinity of NANA is 1000-fold less than that of DANA.

Hence, in order to identify the major species bound in the active site of complex I crystals, we have employed a refinement strategy using three starting models: α-boat NANA (model 1), α-boat NANA omitting O2 (model 2), and DANA (model 3). The restraints on the geometry around C2 were relaxed for each model (for details, see Structure Determination). When models 1 and 2 were used, C2 retained to a large extent its tetrahedral geometry, but there was still no significant density for O2 in the corresponding $\|F_o| - |F_c\|$ difference maps where F_c was calculated using the refined coordinates of NA in complex I. When model 3 was used, C2 clearly moved away from the plane defined by C1, C3, O6 of the starting DANA model. The coordinates from this refinement had the best fit to the $\|F_o| - |F_c\|$ electron density map (Figure 2A, Table 3). When DANA in complex II was refined using the same starting model and restraint relaxations as previously used for complex I, model 3, no significant changes to the DANA geometry occurred in complex II. Therefore, the refined coordinates of complex I, model 3, are clearly different from those of chemically synthesized DANA (Figure 2C, Table 3). Thus, the question is what chemical species are present in the NA active site? Since the occupancy resulting from X-PLOR refinement could not be interpreted as a true measurement of O2 presence in the complex, a series of F_c electron density maps were calculated using the refined model 1 coordinates with arbitrarily assigned O2 occupancies. The F_c electron density map for 20% O2 occupancy appears to be compatible with the $\|F_o| - |F_c\|$ map calculated by use of the

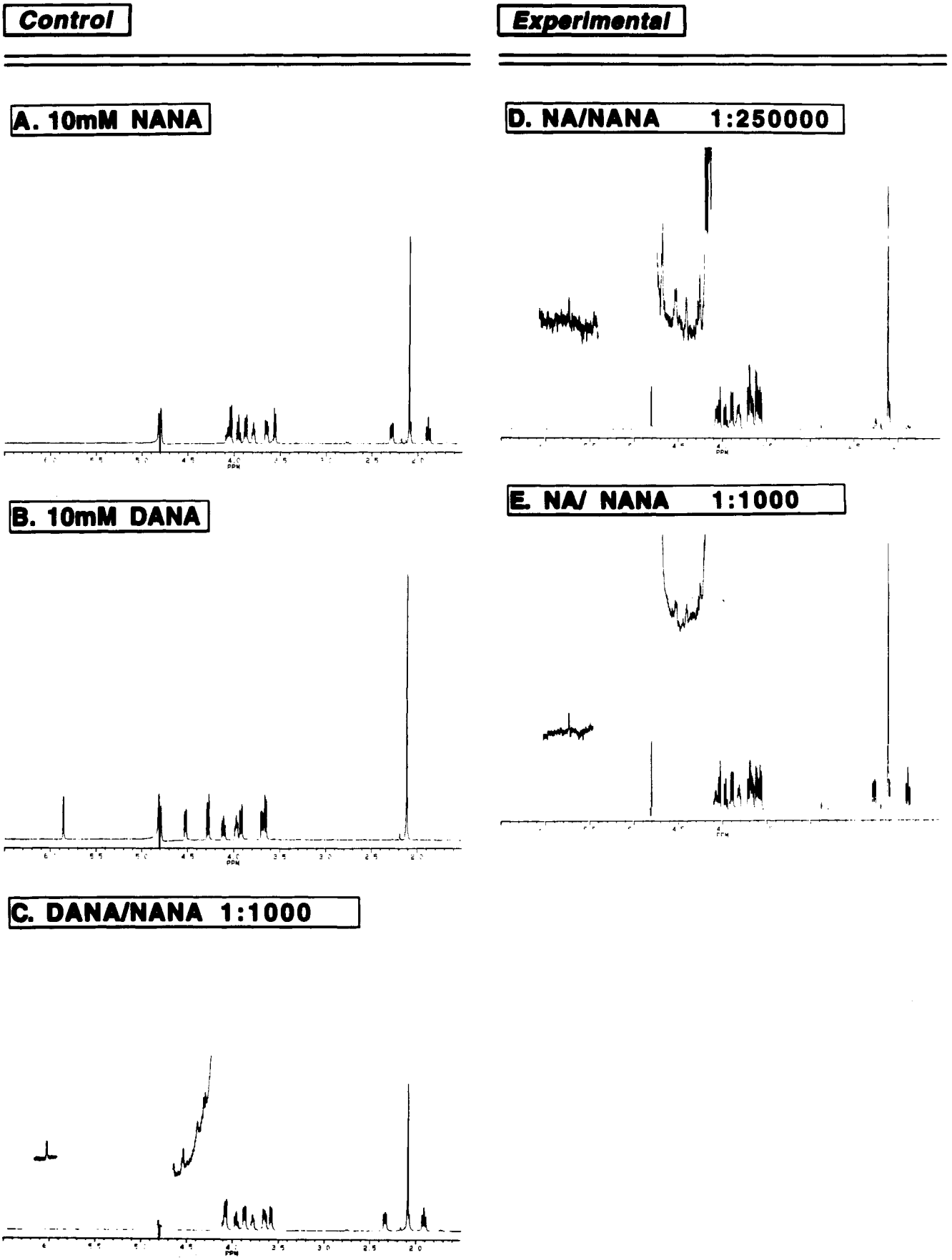

FIGURE 3: NMR analysis of the hydrolysis products of influenza virus neuraminidase B/Lee/40 using NANA (sialic acid) as the substrate. The experimental conditions were specified in the text. (A–C) The control experiments showed that 0.1% of DANA mixed with NANA could be detected by this method. The shifting of the DANA characteristic peaks (e.g., 6.2 to 5.8 ppm) in the mixture could be due to the additional hydrogen bonds of DANA to NANA. (D, E) The experimental data for the given NA/NANA starting ratios indicate that the conversion of NANA to DANA by NA was approximately 0.1% of NANA as judged by comparison of the NANA/DANA peak height ratio in the experimental spectra to the NANA/DANA peak height ratio in the 0.1% DANA/NANA control spectrum.

Table 3: Occupancies, Normalized Electron Densities, and Geometrical Data for NANA and DANA in Their Respective Complexes with NA

	NA–NANA			
	model 1	model 2	model 3	NA–DANA
occupancies[a]				
inhibitor	0.94	0.95	0.99	0.98
O2	0.65			
B-factors, Å^2				
inhibitor	9.46	8.66	9.44	
O2	21.59			
distances, Å[b]				
C2–O2	1.46 (1.41)			
C2–O6	1.38 (1.43)	1.39 (1.43)	1.41 (1.43)	1.37 (1.43)
C6–O6	1.42 (1.43)	1.43 (1.43)	1.43 (1.43)	1.37 (1.43)
C1–C2	1.56 (1.52)	1.55 (1.52)	1.42 (1.38)	1.39 (1.38)
C2–C3	1.55 (1.52)	1.57 (1.52)	1.40 (1.38)	1.41 (1.38)
C3–C4	1.54 (1.52)	1.56 (1.52)	1.56 (1.52)	1.50 (1.52)
angles, deg[c]				
C1–C2–C3	114.30 (108.72)	115.65 (108.72)	124.82 (122.25)	134.02 (122.25)
C1–C2–O6	103.05 (107.24)	102.16 (107.24)	112.48 (118.75)	112.41 (118.75)
O2–C2–C1	106.90 (109.50)			
O2–C2–C3	111.17 (110.10)			
O2–C2–O6	110.40 (111.55)			
O6–C2–C3	110.67 (109.40)	109.09 (109.40)	112.00 (109.40)	111.45 (109.40)
C2–C3–C4	112.53 (110.70)	112.53 (110.70)	120.93 (120.00)	119.39 (120.00)
C2–O6–C6	121.58 (113.80)	121.87 (113.80)	126.53 (113.80)	117.54 (113.80)

[a] Occupancies are with respect to the protein atom occupancy of 1.0. [b,c] The equilibrium distances and angles within parentheses are those parameters employed by X-PLOR.

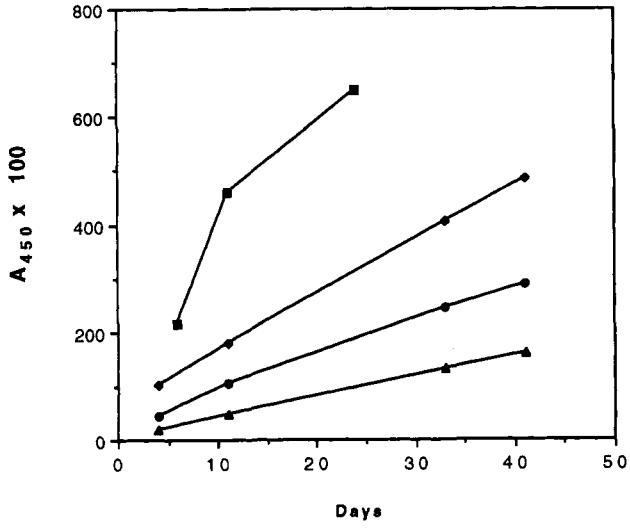

FIGURE 4: Hydration of DANA by influenza virus neuraminidase. Either B/Lee/40 NA at a concentration of 0.5 mg/mL (▲), 1.0 mg/mL (●), and 2.0 mg/mL (♦) or A/tern/Australia/G70c/75 (N9) NA at a concentration of 2 mg/mL (■) was incubated with an initial concentration of DANA (10 mM) at 20 °C. Aliquots were removed at the indicated time points, and the relative amount of NANA in the sample was determined by optical absorbance at 450 nm assaying for NANA as described by Aymard-Henry et al. (1973).

refined model 3 coordinates. Very weak density at the expected O2 position appeared when the contour level was reduced to 0.5σ (Figure 2C). This may be an indication that a low percentage of the bound compound is NANA. Therefore, NANA could only account for 20% or less of the total bound species in the NA active site. If the remaining 80% was DANA, the refined coordinates of complex I, model 3, would have been the same as those of complex II, DANA. The final structure of complex I, model 3, strongly suggests that a third species other than NANA and DANA is bound in the NA active site at a significant percentage. One likely candidate is the NANA-derived oxocarbonium ion, which was shown to be present in the pathway of influenza virus neuraminidase hydrolysis (Chong et al., 1992). The geometry of the refined complex I, model 3, is compatible with that of the postulated oxocarbonium ion.

Mechanism of Action. On the basis of competitive inhibition studies with *Arthrobacter sialophilus* neuraminidase, Miller et al. (1978) postulated that a salt bridge forms between a positively charged group on the enzyme and the carboxylate group of the substrate, which results in the distortion of the substrate to the half-chair conformation and the formation an oxocarbonium ion with a positive charge at C2. Similarly, Chong et al. (1991) showed that a positively charged residue was involved in substrate binding and hydrolysis by an influenza virus neuraminidase (A/Tokyo/3/67). Using site-directed mutagenesis, Lentz et al. (1989) identified amino acids involved in enzyme activity without the full knowledge of the NA three-dimensional structure. Although the enzyme mechanism proposed by Lentz et al. (1989) is incompatible with the three-dimensional structure, the results showed the critical role of at least five conserved active site residues in neuraminidase activity. Recent studies of kinetic isotopic effects by Chong et al. (1992) have provided evidence for the formation of an oxocarbonium ion in the neuraminidase reaction. The prior results implicated that the formation of the oxocarbonium ion at C2 is a key step in neuraminidase hydrolysis, but as yet no mechanism for its induction and stabilization has been proposed that is fully compatible with all the structural, biochemical, and kinetic data.

On the basis of the refined structure of complex I, we propose the enzyme mechanism shown in Scheme 1 for influenza virus neuraminidase. As the sialyl group of the substrate binds to the active site, it undergoes a ring distortion probably due to the strong ionic interactions between the carboxylate of the substrate and the three guanidinium groups of arginines 116, 292, and 374. These conformational changes induce the formation of the strained oxocarbonium ion in the active site which results in the cleavage of the glycosidic bond. The aglycon moiety leaves the active site with the glycosidic oxygen which becomes protonated by solvent. Stabilization of the positively charged oxocarbonium ion could result from keeping the C2 carbonium planar. This is achieved by multiple interactions between the functional groups of the intermediate

Scheme 1

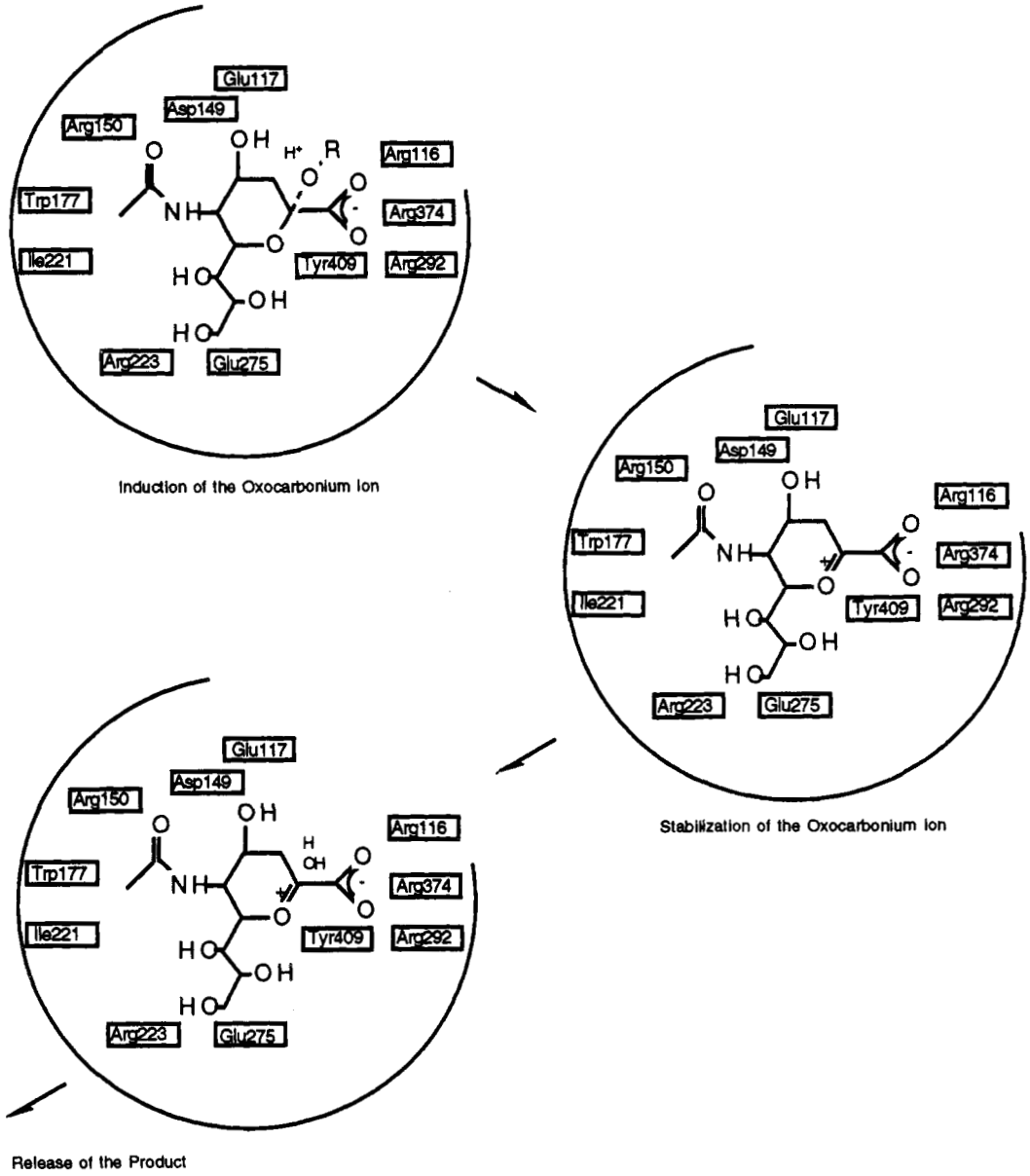

and the active site residues. Such a strong binding is only possible when the C2 atom is in a planar conformation similar to DANA. Although the side-chain carboxylate of Asp149[2] and the partial negative charge on Tyr409 OH (enhanced by hydrogen bonding with Glu276 OE1) could contribute in part to the direct neutralization of the positive charge of the C2 carbonium, their major role in the overall stabilization is to maintain the C2 carbonium ion planarity in the transition state. In the rate-limiting step of the reaction, the oxocarbonium ion picks up a hydroxyl molecule from solvent and leaves the active site as NANA. This mechanism clearly rationalizes the data from site-directed mutagenesis because it requires the participation of all the active site residues in the stabilization of the transition state. It is also consistent with the kinetic isotopic effects which predict the same number of steps in the reaction. Finally, stable binding of the positively charged intermediate by keeping it in a planar conformation must be an inefficient step, and therefore, the mechanism would result in the slow turnover number of 9 s^{-1} which we have measured (data not shown).

[2] Asp149 in B/Lee/40 NA is equivalent to Asp152 in A/Tokyo/3/67.

DISCUSSION

We propose a mechanism of influenza virus neuraminidase reaction in which the driving force comes solely from the induction and stabilization of the oxocarbonium ion intermediate. The activation of the substrate does not involve any nucleophile or proton donor as found in other hydrolases. The stabilization is through concerted interactions between the positively charged intermediate and the active site residues which maintain the planarity of the C2 oxocarbonium intermediate. The suggestion by Burmeister et al. (1993) that the sialyl cation is stabilized primarily by the charge on Tyr409 OH (Tyr408 in B/Beijing/1/87 NA) is inconsistent with the result that mutations of active site residues other than Tyr409, including Asp149 and Glu275, could abolish the enzyme activity. All the active site residues must contribute not only to the binding of the substrate but also to the stabilization of the oxocarbonium intermediate. This is supported by evidence that a newly synthesized analog of DANA which lacks the 4-hydroxyl and 6-glyceryl groups can still bind crystalline NA efficiently without interactions to Asp149 and Glu275 (unpublished data of our ongoing experiments).

The mechanism proposed by Burmeister et al. (1993) also suggested an irreversible production of DANA as a side product by proton elimination at C3 of the oxocarbonium intermediate. In contrast, our experiments showed that DANA was gradually hydrated by influenza virus NA, both types A and B (Figure 4).

ACKNOWLEDGMENT

We are grateful to Drs. Burmeister, Ruigrok, and Cusack, EMBL Outstation, France, for providing the atomic coordinates of B/Beijing/1/87 NA prior to the publication of their work. We thank Mr. Paul A. Demuth and Dr. Mike Jablonsky for help on the NMR studies and Lily Yang for help in making Figure 2. Excellent technical assistance was provided by Aulikki Koskinen.

REFERENCES

Aymard-Henry, M., Coleman, M. T., Dowdle, W. R., Laver, W. G., Schild, G. C., & Webster, R. G. (1973) *Bull. W.H.O. 48* (2), 199–202.

Brunger, A. T. (1992) *X-PLOR Version 3.0 Manual*, Yale University, New Haven, CT.

Bucher, D., & Palese, P. (1975) in *The Influenza Viruses and Influenza* (Kilbourne, E. D., Ed.) pp 83–123, Academic Press, New York.

Burmeister, W. P., Ruigrok, R. W. H., & Cusack, S. (1992) *EMBO J. 11*, 49–56.

Burmeister, W. P., Henrissat, B., Bosso, C., Cusack, S., & Ruigrok, R. W. H. (1993) *Structure 1*, 19–26.

Carson, M., & Bugg, C. E. (1986) *J. Mol. Graphics 4*, 121–122.

CCP4 (1979) *The SERC (U.K.) Collaborative Computing Project No. 4, A Suite of Programs for Protein Crystallography*, Daresbury Laboratory, Warrington, U.K.

Chong, A. K. J., Pegg, M. S., & von Itzstein, M. (1991) *Biochem. Int. 24*, 165–171.

Chong, A. K. J., Pegg, M. S., Taylor, N. R., & von Itzstein, M. (1992) *Eur. J. Biochem. 207*, 335–343.

Hendrickson, W. A., & Connert, J. H. (1981) in *Structure, Conformation, Function and Evolution* (Srinivasan, R., Subramanian, E., & Yathindra, N., Eds.) pp 43–57, Pergamon Press, Oxford.

Howard, A. J., Gilliland, G. L., Finzel, B. C., Poulos, T. L., Ohlendorf, D. H., & Salemme, F. R. (1987) *J. Appl. Crystallogr. 20*, 338–387.

Jones, T. A. (1985) *Methods Enzymol. 115*, 157–171.

Lentz, M. R., Webster, R. G., & Air, G. M. (1987) *Biochemistry 26*, 5351–5358.

Lin, Y., Luo, M., Laver, W. G., Air, G. W., Smith, C. D., & Webster, R. G. (1990) *J. Mol. Biol. 214*, 639–640.

Meindl, P., Bodo, G., Lindner, J., Palese, P. (1971) *Z. Naturforsch. 263*, 792–797.

Miller, C. A., Wang, P., & Flashner, M. (1978) *Biochem. Biophys. Res. Commun. 83*, 1479–1487.

Rossmann, M. G., & Blow, D. M. (1962) *Acta Crystallogr. 15*, 24–31.

Varghese, J. N., McKimm-Breschkin, J. L., Caldwell, J. B., Kortt, A. A., & Colman, P. M. (1992) *Proteins 14*, 327–332.